ELSEVIER

Nuclear Engineering and Design 146 (1994) 83–95

Nuclear Engineering and Design

Multiphase transients in the premixing of steam explosions

S. Angelini *, E. Takara *, W.W. Yuen *, T.G. Theofanous

University of California, Santa Barbara, Center for Risk Studies and Safety, Department of Chemical and Nuclear Engineering, Santa Barbara, CA 93106, USA

Abstract

This paper describes the first attempt to experimentally quantify the multiphase transient associated with the premixing of steam explosions – a hot particulated (heavy) phase falling, in film boiling, into a coolant pool, which is thus forced to rapid vaporization. The process is characterized by mixing-zone-averaged and local void-fraction transients, as well as mixing-front advancement histories, and the data are found to be in good agreement with predictions carried out with our PM-ALPHA code. In particular, these tests confirm the predicted water depletion phenomenon which is a crucial factor in limiting the energetics of large-scale steam explosions.

1. Introduction

Essentially all practically relevant steam explosions occur in the pouring mode of contact. Large, energetic explosions can only evolve from (or propagate through) "adequately" dispersed states created in this pouring/mixing process. In analogy with chemical explosions these states are referred to as "premixtures". A premixture is characterized by the spatial distribution of the "reactants", the "hot" and "cold" liquids (alternatively referred to as "fuel" and "coolant") and a third "inert" component, the "vapor". The role of this third component is dual: first, it introduces compressibility which has a dissipative effect on triggering, escalation and propagation of an explosion; second, it implies depletion of liquid coolant (the "working" fluid) and thus reduced energetics even if an explosion were to occur. This latter aspect was first recognized by Henry and Fauske [1], and it was a key ingredient in the quantification of steam-explosion-induced containment failure by Theofanous et al. [2]. These initial predictions were made with a transient, two-dimensional, two-fluid model, i.e., with the assumption that the vapor and liquid coolant behave as a homogeneous-equilibrium mixture. In subsequent work [3] this assumption was relaxed by the use of a three-fluid model, which produced similarly-depleted (in water) premixtures. Clearly, it is important that these predictions are confirmed experimentally.

This experimentally-oriented effort consists of three parts. The first is to examine the interface transfer laws (the so-called "closure" relations) in three-phase systems, with the one phase in film boiling. Initial results have been reported by Liu et al. [4]. The second effort is to examine the integral aspects of the premixing process with emphasis on the performance of the three-fluid modelling approach. For this purpose we use an already particulated hot mass (particles of a given

* Also with the Department of Mechanical and Environmental Engineering.

SSDI 0029-5493(93)E0222-6

size) instead of a liquid, and seek to characterize in detail the spatial-temporal evolution of the three-phase mixing zone created when these particles are dumped (as a cloud) into a liquid coolant pool. This is the subject of this paper. Finally, the third effort is to test the prediction in experiments, run with molten "fuel" thus including the "fuel" break-up phenomena during premixing. It is expected that the FARO experiments at the European Joint Research Center (Ispra) and the ALPHA experiments at the Japan Atomic Energy Research Institute (Tokai) will provide data adequate for this purpose. It should be mentioned, however, that, by its very nature, the breakup process can only be indirectly inferred from these experiments (i.e., vapor production rates), and it is expected to remain uncertain in its details – nevertheless, its effect on the water-depletion phenomenon, and thus on energetics, can be bounded by parametric evaluations.

2. Experimental facilities

The basic concept of the experiment (called MAGICO) is illustrated in Fig. 1. Tens-of-kilograms quantities of mm-size steel balls are heated to a uniform high (up to 1000°C currently) temperature, then transferred into an intermediate container equipped with a dumper mechanism, and within a few seconds are released into a pool of saturated water in a lower-plenum-like geometry. The intent is to match (except for the breakup) the water- depletion regimes of the reactor in a 1/8-scale geometry, and numerical simulations (PM-ALPHA) are used for this purpose. The

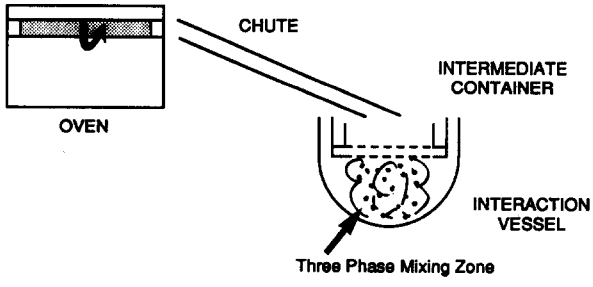

Fig. 1. Schematic of the MAGICO experiment.

major experimental parameters are: particle size, particle temperature, pour diameter and particle entry velocity. In addition, we intend to vary the particle cloud density and the lower plenum geometry (by including internal structures). In the following we provide some details of the experimental equipment and the measurement techniques.

For this experiment the oven cavity was equipped with a ceramic cylinder (1.67 m long, 8.2 cm in diameter) that could be loaded, plugged at both ends, and rotated during heating to prevent the steel balls from sticking together at high temperatures. The rotation also helped obtain temperature uniformity. Integrity of the ceramic cylinder requires that heat-up be regulated closely at less than 150°C per hour – 13 hours are required for a 1000°C run, including cooldown. When the desired temperature level is reached, the one end of the cylinder is unplugged, and the whole oven is tilted so that by gravity flow the balls are transferred to the intermediate container (this process lasts about 2 min.). Future tests with aluminum oxide particles will allow temperatures up to the maximum oven capacity, which is 1400°C. The intermediate container (21 cm in diameter) is equipped with several thermocouples located such as to allow a good characterization of the initial temperature of the particulate at the moment it is released. Both the nominal (initially in the oven) temperature and this, actual, temperature are recorded, and typically they differ by less than 100°C. Sudden and uniform release is achieved by a solenoid-operated air-cylinder operation that, by a slight movement, aligns the holes of two perforated plates that make up the bottom of the intermediate container. In the present set-up, the holes are 1.1 cm in diameter, placed on a square 1.27 cm pitch. In future tests this pitch will be varied to obtain different cloud densities. The maximum pour diameter is 20 cm.

The lower plenum scale model (the interaction vessel) was fabricated from steel and is equipped with an observation window. Preliminary tests indicated that the behavior is quite similar to that obtained in a plain rectangular vessel (406 mm on the side, with a height of 355 mm), and the use of

such (made of tempered glass) was made, in the experiments reported herein, to allow easy and complete visualization. The whole experimental setup is shown in Fig. 2. Not discernible are the FLUTE components (see next section) as they are located just behind the interaction vessel. Not shown is the data acquisition system which is located in another room.

3. Measurement techniques

As mentioned above, the key measurement in these experiments is the space-time evolution of the volume fractions, in the two-dimensional evolving mixing zone, during the short (less than 1 s) transient. [An indication of what is involved is given in Fig. 3]. Such measurements were made at the global level; that is, averages over the whole mixing zone, as well as at the local level; that is, on a sample volume of $\sim 1/4$ cm^3 at several locations within the mixing zone. The presence of hot particles introduced a different sort of difficulty for each of these two measurement approaches – correspondingly they were susceptible to different kinds of limitations. This made them complimentary to each other, specifically with regards to the portion of the transient (earlier vs. later) best suited to each. Each measurement is discussed further below.

Since the melt volume fraction in the mixing zone is less than 2% (this is estimated from the pour area and the particle delivery rate, and is consistent with the results of PM-ALPHA calculations) the liquid (water) volume fraction in it can be deduced from measurements of the zone-averaged void fraction. By mass continuity this can be related to the apparent increase in volume of the surrounding liquid which, in turn, can be obtained from the observed level rise. Such data were obtained throughout the transient by closeup high speed movies (camera #1 in Fig. 2). In addition, the whole interaction vessel, and especially the whole free liquid surface, were observed with high speed camera #2. Void fraction data were reduced in two different ways. One referred the measured void volume to the whole mixing zone volume, while the other made use of the whole volume under the pour area (a cylinder with a cross section the same as that of the pour area and a height equal to the instantaneous height of the liquid in the interaction vessel). The first will be referred to as "mixing-zone-averaged" void fraction, while the latter as "pool-height-

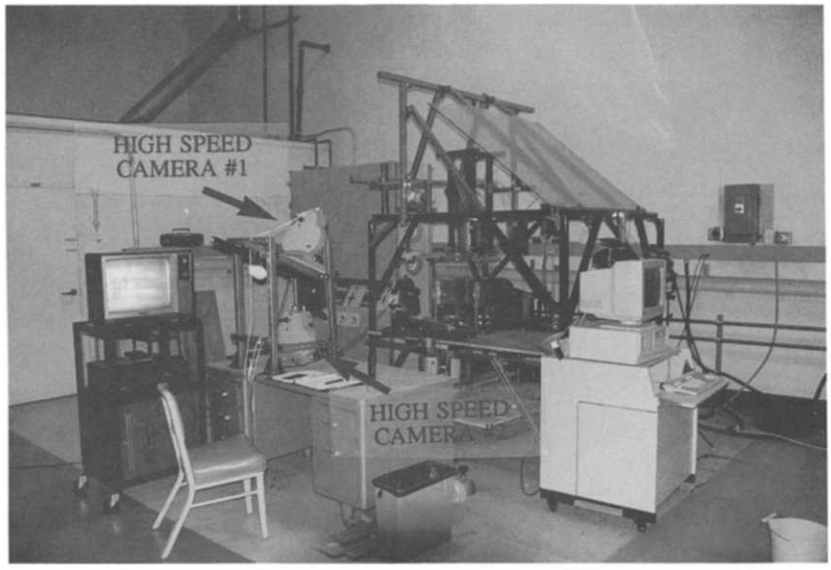

Fig. 2. An overall view of the MAGICO experimental setup.

averaged" void fraction. Clearly, the two should agree when the melt-front just touches the pool bottom and begins to accumulate on it. As seen in Fig. 3, the mixing zone maintains the cross section of the pour area, thus for the "mixing-zone-averaged" void fraction the mixing zone front only needs to be tracked. The error in estimating the water position is ± 1 mm, thus the "pool-height-averaged" void fraction data involve an absolute error of $\pm 2\%$. The "mixing-zone-averaged" void fraction measurement uncertainty is primarily impacted by properly following the mixing zone front. It is estimated that this was done to within ± 1 cm, which translates to a rather significant error initially, decreasing gradually to about $\pm 10\%$ (relative error) near the end. Errors due to air entrained with the particles are negligible as verified by pours of cold particles that produced no measurable level rise. At still later times, the interface breaks up in the manner illustrated by the third snapshot in Fig. 3. This often happens at around the time the mixing-zone front reaches the pool bottom, but sometimes earlier also. Clearly, this marks the end of the time period for this sort of data.

From a practical standpoint, this is also the

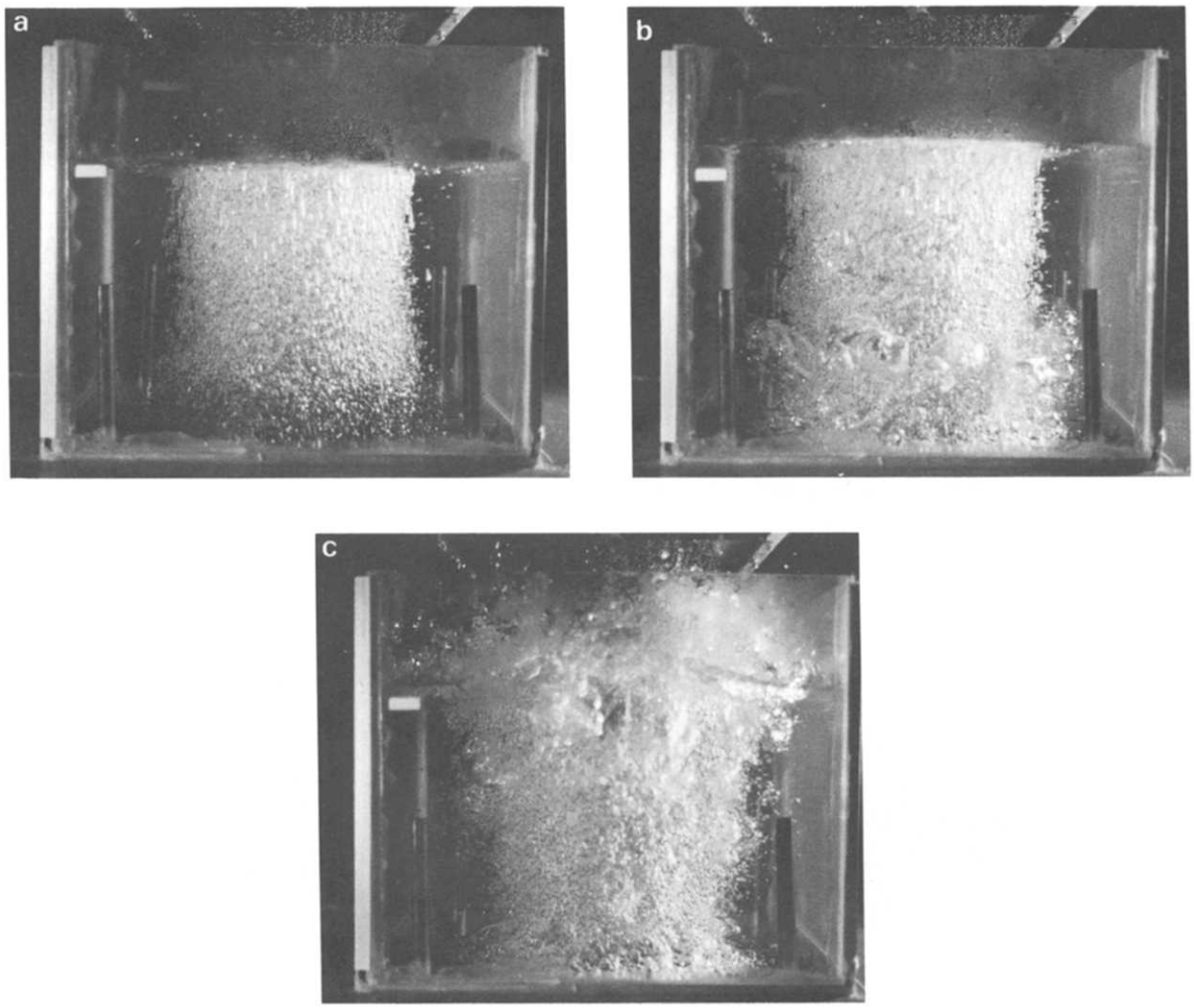

Fig. 3. Snapshots of a typical premixing transient in MAGICO. The times are 0.27, 0.57, and 0.87 s.

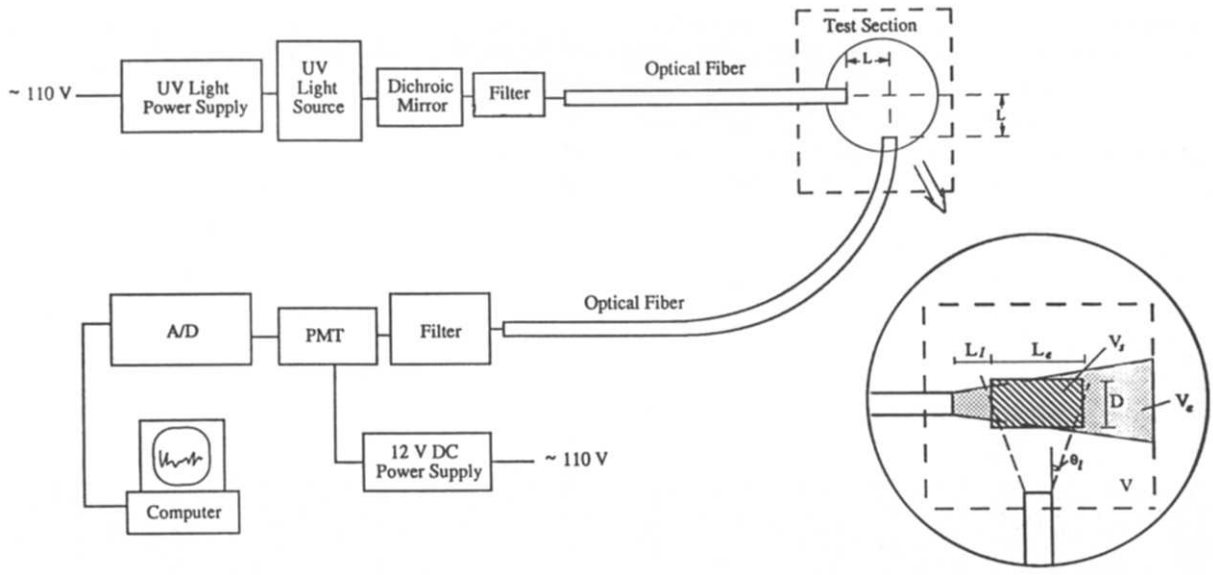

Fig. 4. Schematic illustration of FLUTE. The measurement volume is V_s.

time period of interest for steam explosion energetics – if an explosion has not been triggered up to this point, it should be at the point of impact, rather than at any later time. Still, it is interesting to follow the void fraction transient for somewhat longer. The local void fraction measurement besides providing the local structure is complementary to the volume-averaged one also in this respect.

Even though less than 2% by volume, the presence of the hot, solid particles present serious difficulty in the measurement of local liquid

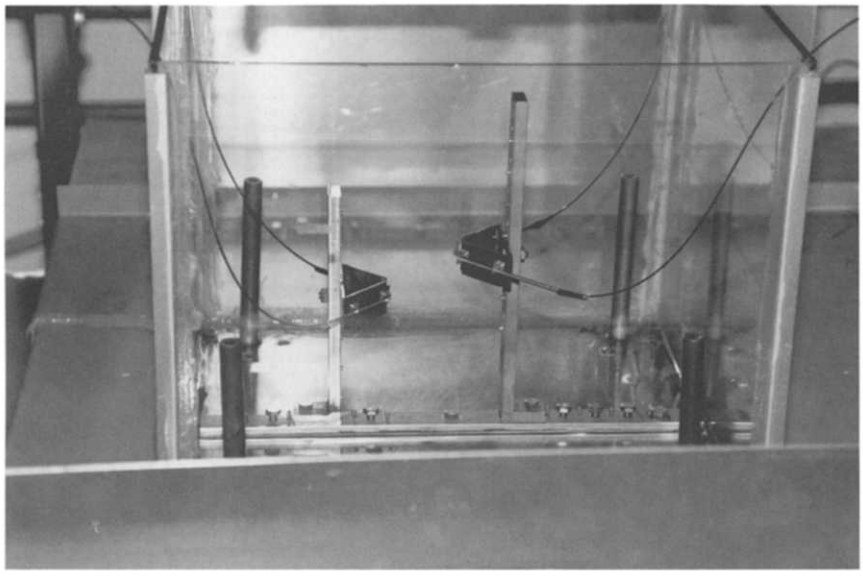

Fig. 5. The FLUTE fibers and supports for two simultaneous measurement locations in the interaction vessel.

Table 1
Experimental matrix for runs with global liquid fraction measurement (1.5 mm chrome-alloy AISI-52100 particles)

Run #	Oven temperature (°C)	Particle temperature (°C)	Pool depth (cm)	Free fall distance (cm)	Pour diameter (cm)
101	600	560	25	15	20
102	800	750	25	15	20
103	1000	880	25	15	20
104	600	600	15	15	20
105	600	580	15	25	20
106	800	720	15	15	20
107	600	560	25	5	20
108	1000	800	15	15	20
109	1000	860	15	25	20
111	800	760	15	25	20
112	800	760	25	5	20
113	600	600	25	15	12
114	800	760	25	15	12
115	600	600	15	15	12
116	800	780	15	15	12

(void) fractions. A new instrument, FLUTE, had to be invented for this purpose [5,6]. The principle of this measurement can be explained with the help of Fig. 4. The idea is to measure the intensity of fluorescent light emitted from a local fluid region, activated by ultraviolet radiation (a dye, fluorescein, dissolved in the liquid being the active ingredient). The size of the measurement volume is controlled by the distance L between the fibers (the acceptance θ_f angle is 29°). Be-

Table 2
Experimental matrix for runs with local liquid fraction measurement (2.4 mm stainless steel particles, 25 cm pool depth, 20 cm pour diameter, and free-fall distance 15 cm, except Runs #204 and #401, set at 5 cm and 3 cm, respectively)

Run #	Oven temperature (°C)	FLUTE position #1			FLUTE position #2		
		H (cm)	R (cm)	L (mm)	H (cm)	R (cm)	L (mm)
204	800	17.5	0	5	19	2.5	5
209	600	20	3.4	4	16.5	3.4	4
210	600	20	3.4	4	16.5	3.4	4
211	800	20	3.4	4	16.5	3.4	4
301	600	20	3.4	4	19	3.4	4
302	600	20	3.4	4	19	3.4	4
303	600	20	3.4	4	19	3.4	4
304	600	20	3.4	4	19	3.4	4
305	600	20	3.4	6	19	3.4	2
401	600	20	3.4	2	19	3.4	2
402	600	20	3.4	2	19	3.4	2
403	600	20	3.4	1	19	3.4	1
404	600	20	2.5	1	19	2.5	1
406	600	9.5	3.4	5	8.8	3.4	5
407	600	20	3.4	5	19	3.4	5
408	800	20	3.4	4	19	3.4	4
603	600	20	3.4	4	19	3.4	4
604	600	20	3.4	4	19	3.4	4

Note: H = height from vessel bottom, R = radial distance from centerline

cause the fibers are very fine (1 mm in diameter) their presence provides hardly any disturbance to the flow. For this application (because of the hot, solid particles) the fibers are protected by very fine steel tubing, and they also need to be securely supported, as illustrated in Fig. 5. The supports are made to offer minimal cross-sectional exposure in the main flow direction, and we believe that the disturbance introduced by their presence is insignificant. The data rate is limited only by the capability of the data acquisition system. In the present configuration, this is 8 kHz, but an upgrade to 80 kHz is readily possible.

This instrument offers a unique capability, in general, for the measurement of local, essentially instantaneous, liquid volume fractions in highly transient, multidimensional, dispersed two phase flows. In the present application, the solid particles introduce some additional consideration with regard to the choice of fiber spacing (L in Fig. 4). Particle interference with both the emitting and receiving light beams increases with L (Note, however, that such interference is not present from vapor and gas/liquid interfaces [6]). From numerical simulations (Monte Carlo type) we find that for $L = 4$ mm, a melt volume fraction of 2%, and very low void fractions, this interference leads to a *maximum* absolute error in void fraction of about 10%. That is, for real void fractions of ~ 10%, the FLUTE reading may be as high as

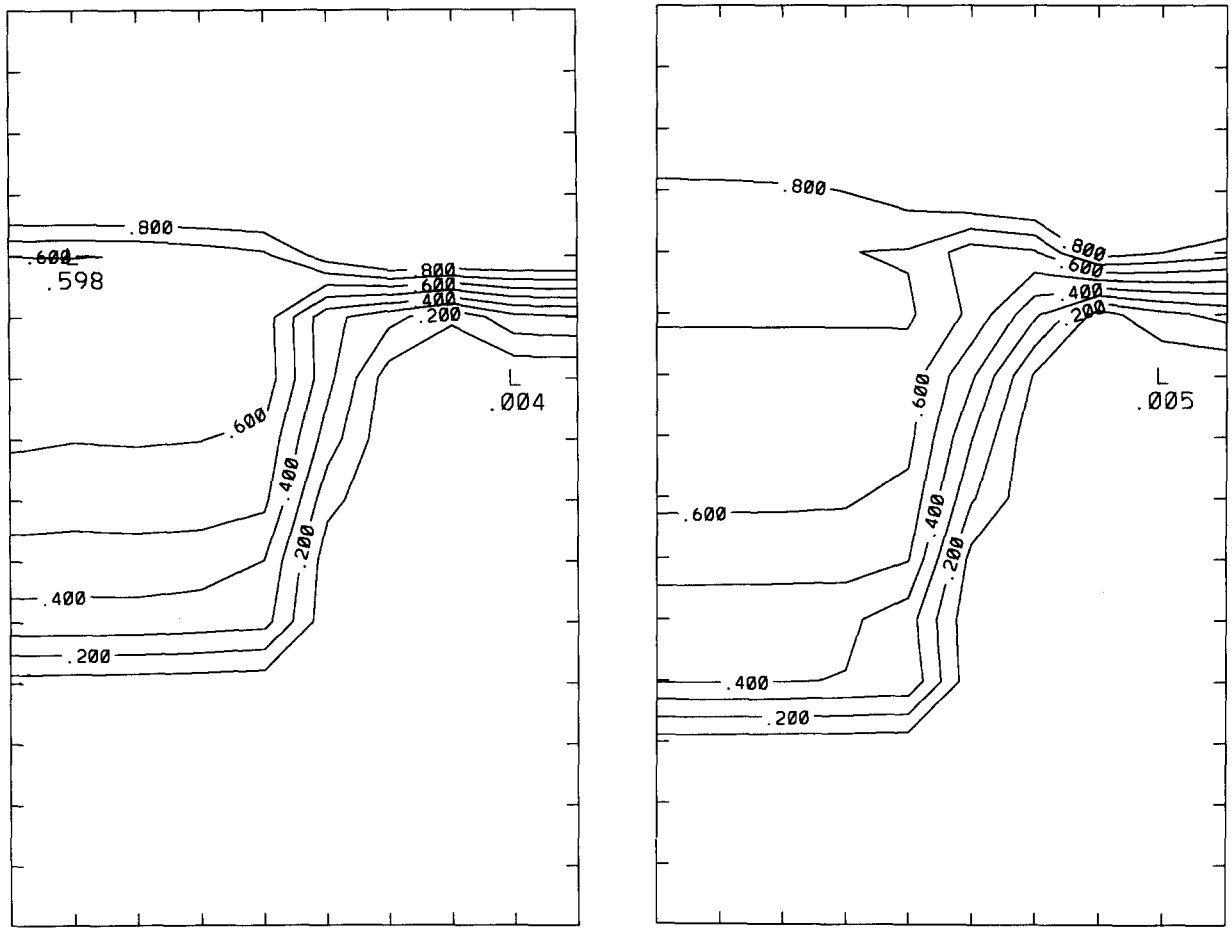

Fig. 6. Calculated development of mixing zone and void fraction distributions in it for the conditions of Run #102 at times of 0.35, 0.40, 0.45, and 0.50 seconds following the initiation of the release.

20%. However, as the void fraction increases, diminishing portions of the particle interference are attributable to a quantity of liquid "shadowed" and thus the absolute error decreases. As a consequence, we expect that the relative error at void fractions over 30% to be under 10%. It is noted, however, that some further work is required to firm up these estimates. On the other hand, as this interference effect is diminished by reducing L, liquid "trapping" between the fibers can lead to errors. We call this fiber interference; it tends to produce erroneously higher values of liquid fraction. From experiments, we found this error to be significant for $L = 1$ or 2 mm. Thus, the measurements reported here were made with $L = 4$ or 5 mm.

In any case, it should be recognized that these are first and unique (at this time) measurements, with a brand new instrument, and clearly in need of further verification. One aspect of this is possible by the order-of-magnitude comparisons with the mixing- zone-averaged measurements, and by more detailed comparisons of both sets of measurements with numerical simulations (PM-ALPHA). A further attempt at such verification is currently made by the use of X rays.

4. Experimental results and interpretations

High-speed movies require very strong illumination of the interaction vessel which interferes

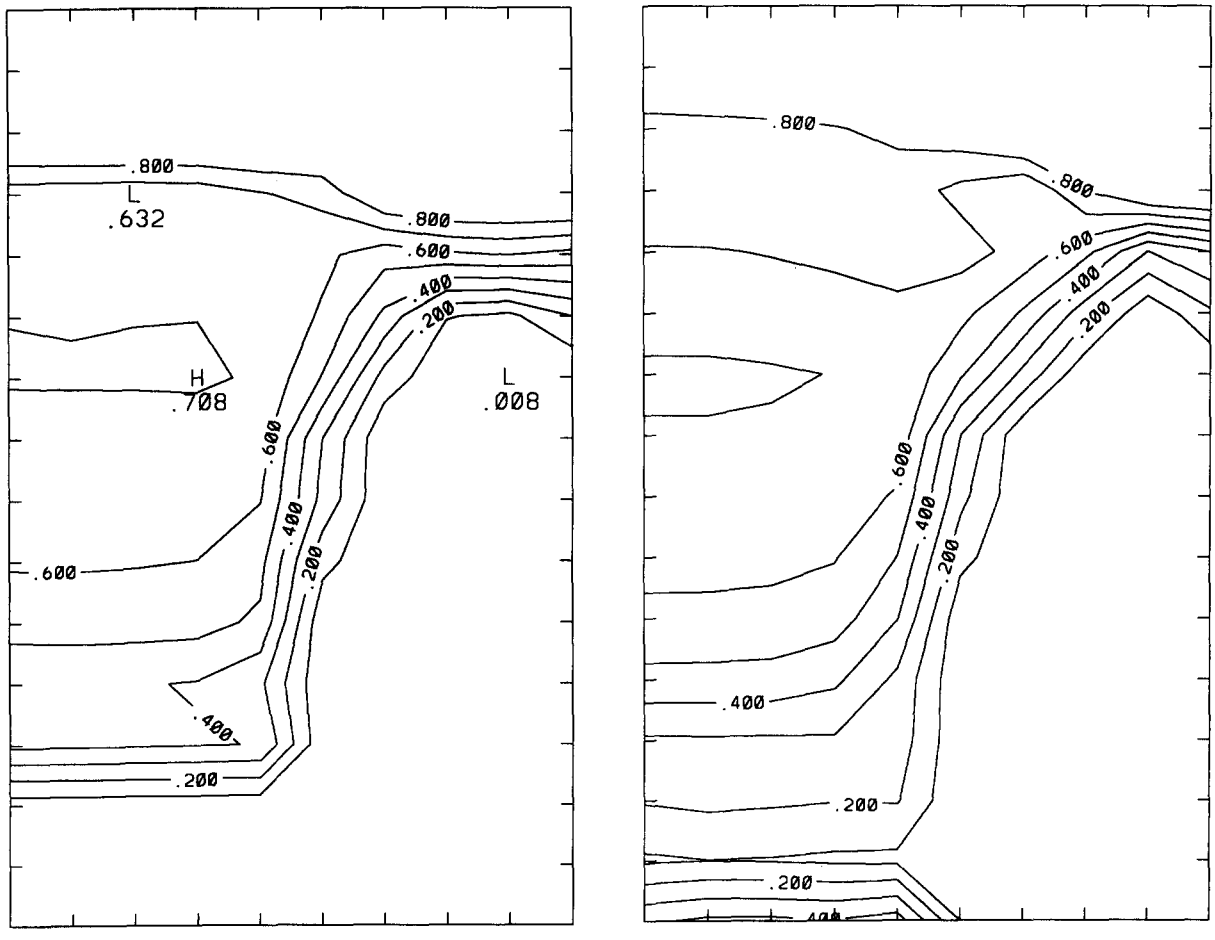

Fig. 6 (continued).

with the fluorescent light measurement in FLUTE, thus the runs with high speed movies were carried out as a separate series. Run numbers and respective experimental conditions have been listed separately for the two sets of runs in Tables 1 and 2. From Table 1 it can be seen that nominal particle temperatures varied in the 600 to 1000°C range (the particle temperatures quoted in this table are those measured in the intermediate vessel just prior to the initiation of the pour); the rest of the experimental matrix covered variations in pour diameter, pool depth, and freefall distance. The freefall distance refers to the distance between the particle release point and the pool surface – this variation creates different particle velocities at the point of pool entry. In the FLUTE runs (Table 2) the main effect studied was the fiber spacing, but other variations included were particle temperature and measurement position.

In all runs the water was at saturation – it was brought to a boil by 4 immersion heaters located at 4 corners in the interaction vessel (these heaters are visible in Fig. 3).

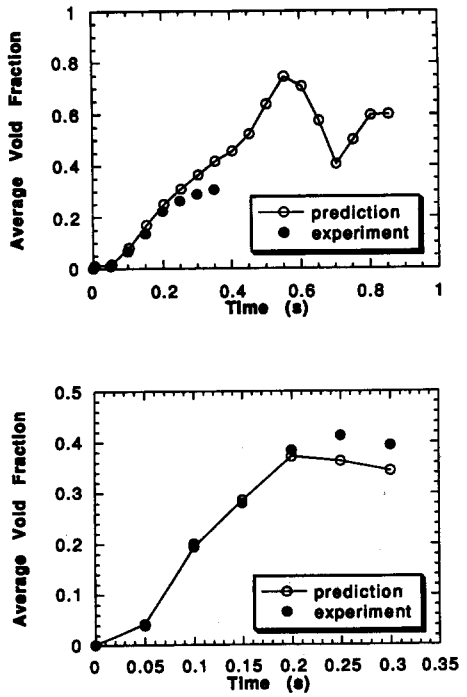

Fig. 7. The pool-depth-average (top) and mixing-zone average (bottom) void fraction transients for Run #102.

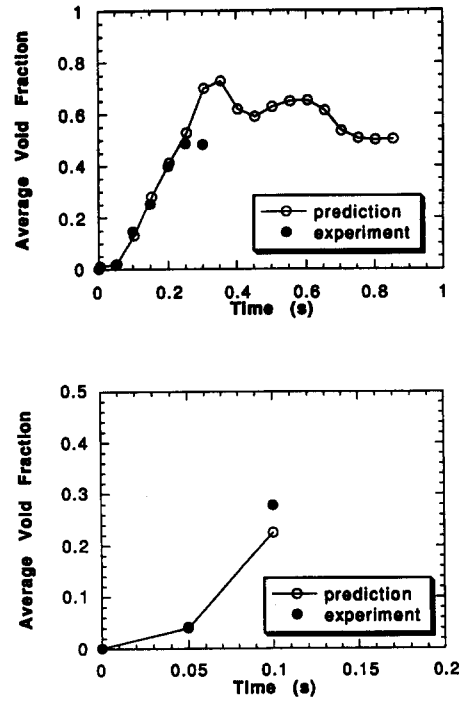

Fig. 8. The pool-depth-average (top) and mixing-zone average (bottom) void fraction transients for Run #106.

In the following, the experimental results are presented in conjunction with predictions using the PM-ALPHA code. The three-fluid formulation used in this code and the set of constitutive laws in it have been completely specified [3]; the predictions are made on this basis. The flow field (which includes the freefall space) was discretized by 2.5 cm (axial) by 2 cm (radial) nodes, in axisymmetric cylindrical geometry (the radial dimension was chosen to represent the interaction vessel cross-sectional area). The particle velocity at the point of release (inlet to the flow fields) was obtained from the high speed movies as 72 cm/s, and it was found to be independent of the quantity of material in the intermediate vessel (presumably the particles' sliding against each other as they enter the holes in the bottom of the intermediate vessel controls the release rate). The particle volume fraction in the same location was found from volumetric release rate of particles to

be 1.87% and 2.5% for the 2.4 and 1.5 mm balls, respectively. In the calculations, the two-phase zone front lagged the particle front by about 3 nodes. To check for numerical diffusion we implemented also a Langrangian treatment, as a side to the main calculation, and the results were found to be in good agreement with both the calculated Eulerian particle front and the particle front motion obtained from the movies.

From such numerical simulations, the two experimentally deduced void fraction transients were computed for the conditions of each experimental run – these are the "predictions" shown with the experimental data in what follows. An illustration of the calculated developing of the mixing zone and the void fraction distributions in it may be seen in Fig. 6. Note that the qualitative features are similar to those of Fig. 3, although maybe somewhat more pronounced.

The complete set of results may be found in Theofanous et al. [7]. Representative results only are included here.

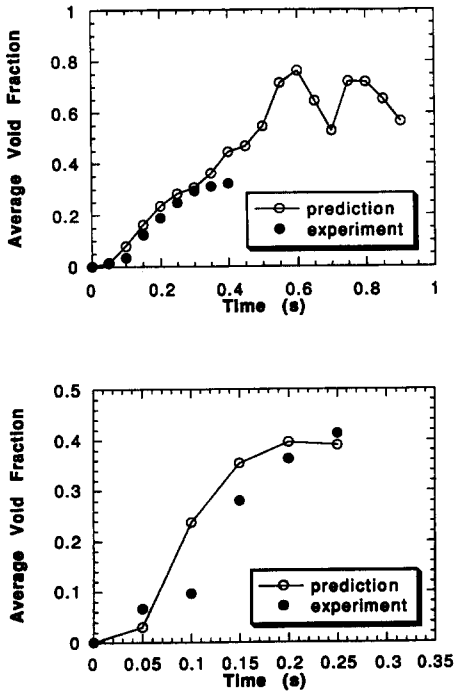

Fig. 9. The pool-depth-average (top) and mixing-zone average (bottom) void fraction transients for Run #112.

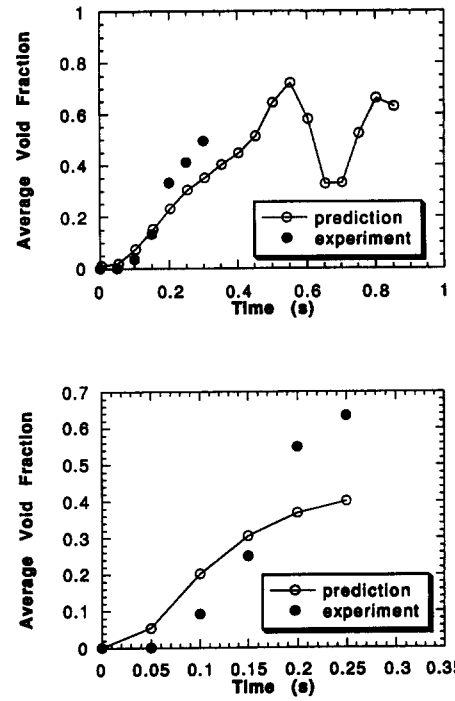

Fig. 10. The pool-depth-average (top) and mixing-zone average (bottom) void fraction transients for Run #113.

Mixing-zone-averaged and pool-height-averaged results from four typical runs in the 100-series are shown in Figs. 7 through 10. As may be seen in Table 1, these illustrations cover the effects of particle temperature, pool depth, freefall distance, and pour diameter. The mixing zone average results extend roughly up to the time that the zone front reaches the pool bottom (note that for the shallow pool run #106 the time scale of the data is about one-half of that for the other three runs). The calculation shows an initial rapid increase and an eventual leveling off in the void fraction as the pool bottom is approached. This is because at higher void fractions steam is able to vent off the top (see Fig. 6), there is less water "feeding" the mixing zone at its front, and heat transfer (and vaporization) degrade because of increase in void fraction. Note that the radiation component of the heat transfer at these particle temperatures is not as strong as what would be expected for the very high temperature fuel in reactor situations. In general, these trends

are born out by the experimental data, with the only notable exception, possibly, the case of run 113. In this run the pour was ~ 1/3 that of the other three runs, and the same trend of significantly higher void fractions at the tail end of the transient was also observed in the other runs (114, 115, 116) of this group. The reason for this difference remains to be clarified. Turning next to the pool-height-averaged void fractions, which also are shown in these figures, we note that the numerical results show initially a rapid rise, but peak and "level off" within a short time after the particles begin to accumulate at the pool bottom. An oscillatory structure, of varying amplitude, on this "level" part is also observed. The experimental data are seen to reveal clearly this early rising trend, but unfortunately they stop short of the peak – as explained earlier, this sort of measurement is not possible after the pool surface begins to break up. This is where the local measurements are very helpful, and they are discussed next.

At 8 kHz, FLUTE provides essentially instantaneous readings of the local liquid fraction – because the sampling volume is so small, the signal often shows either 100% liquid or 100% vapor. These readings were time-averaged over 10, 20, and 50 millisecond time intervals while "sliding" on the time axis. The results for two runs with measurement positions at 2 different depths (see Table 2) are shown in Figures 11 and 12. An additional reduction was performed by averaging the so-smoothed results from 9 different runs (2 equivalent FLUTE positions in 7 of these runs), and these results are shown in Figure 13. The FLUTE signals show the first arrival of the hot particles by the interference signals already discussed in Section 3. Synchronization between the experimental and predicted traces is accomplished by establishing coincidence of this instance to the arrival of the hot particles at the measurement location in the calculation. We see in the measurements a rather complicated struc-

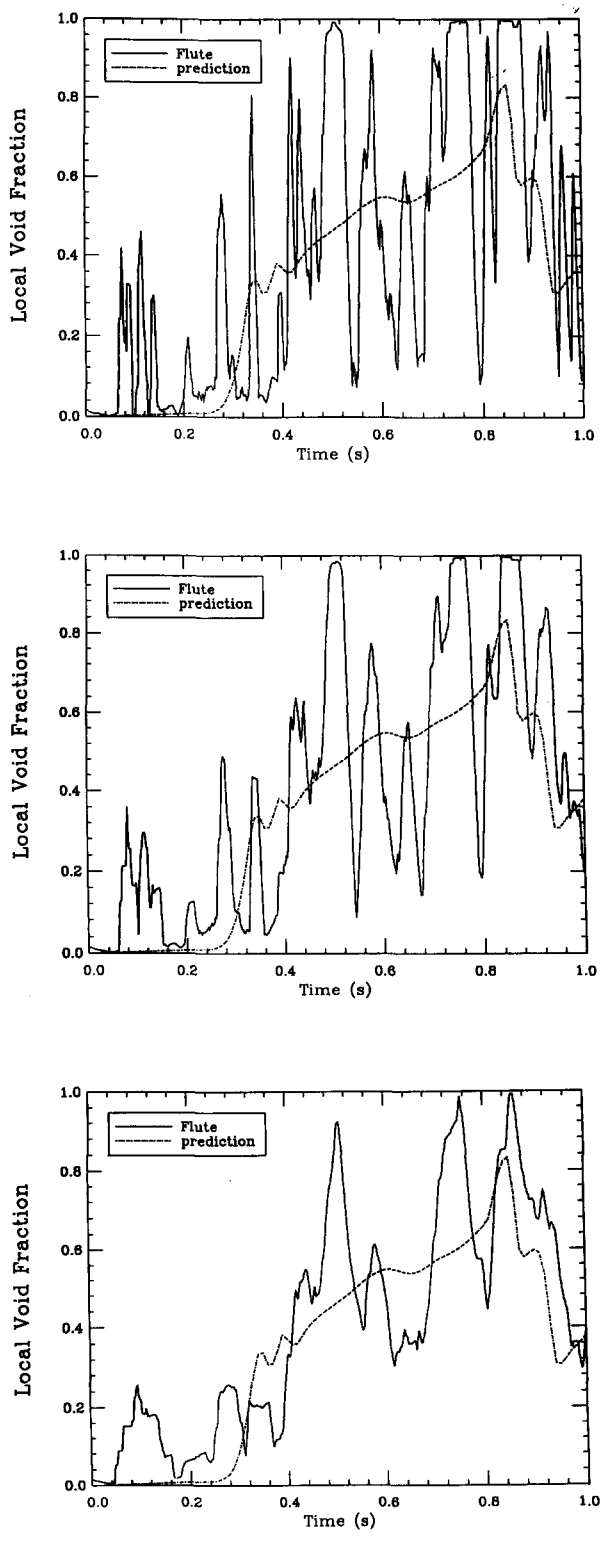

Fig. 11. The local void fraction transient for Run #301 position #1, as deduced by 10 (top), 20 (middle), and 50 (bottom) millisecond time-averaging of the 8 kHz FLUTE signal.

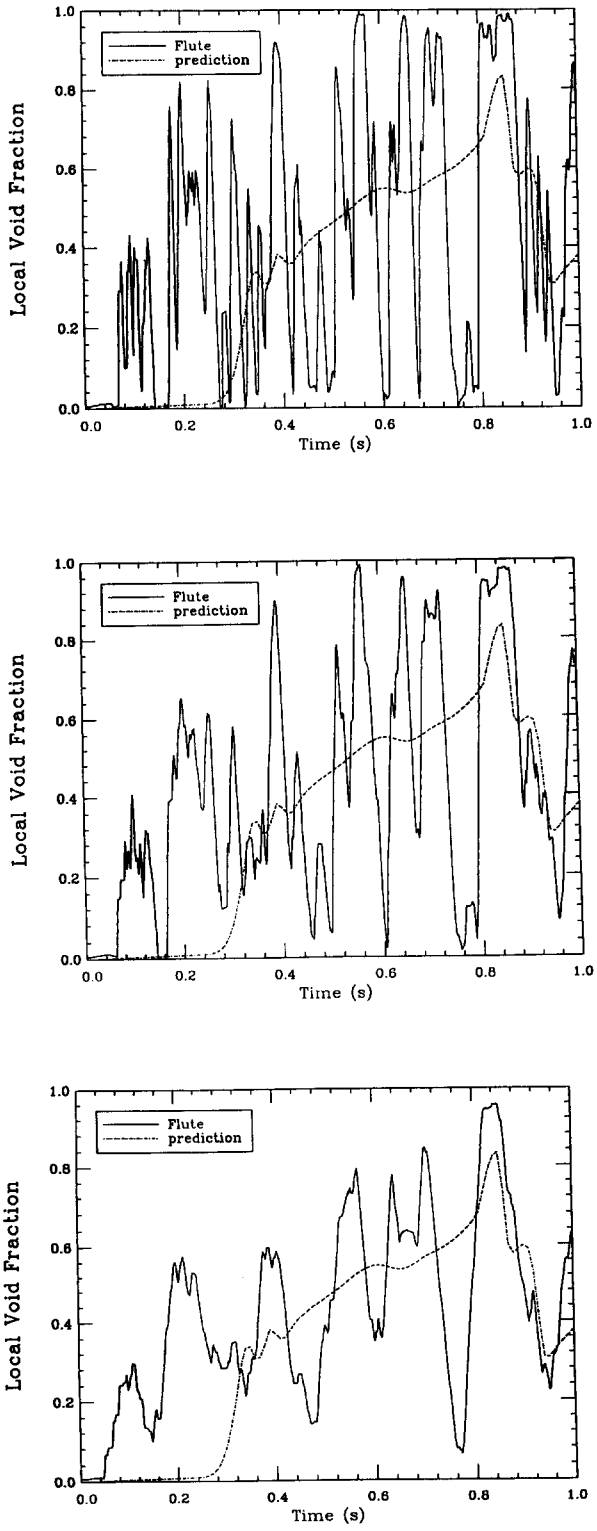

ture, but the general trends are consistent with the predictions. This is particularly evident in the multi-run, or ensemble, average as indicated in Fig. 13. More specifically, in the calculation we observe an initial rapid rise when the two-phase front reaches the measuring location, a more moderate increase for a period of time well past the particle arrival time at the pool bottom and a short and sharp peak followed by a rather marked fall. In the experimental data, the initial rapid rise is somewhat marred by the fiber interference; however, it is still quite evident. Note that this early period is well covered by the global void fraction data discussed above. More clear is the intermediate period of moderate rise. As noted already, in this range of high void fractions the interference error is reduced drastically, and this is very important because we thus extend the measurements into the region for which the global void fraction measurements were not possible. It is also very interesting to note that in the overlapping region there appears to be good consistency between these two measurements. Finally, at the very end of the transients shown, the data do not exhibit as pronounced a fall-off as found in the prediction; indeed, even discerning such a fall-off in the data is rather subjective.

5. Conclusions

An experimental facility and related experimental techniques have been demonstrated to provide a viable vehicle for the study of the extremely complex multiphase zone created by the interaction of a hot particulated phase poured into a volatile liquid. Initial indications are that the process is dominated by heat transfer and the resulting vapor production, in general, is not sensitive to details of the phenomenology. Comparison with predictions made by using the PM-ALPHA code are encouraging. At this time, the experimental data and related computations pre-

Fig. 12. The local void fraction transient for Run #406 position #1, as deduced by 10 (top), 20 (middle), and 50 (bottom) millisecond time-averaging of the 8 kHz FLUTE signal.

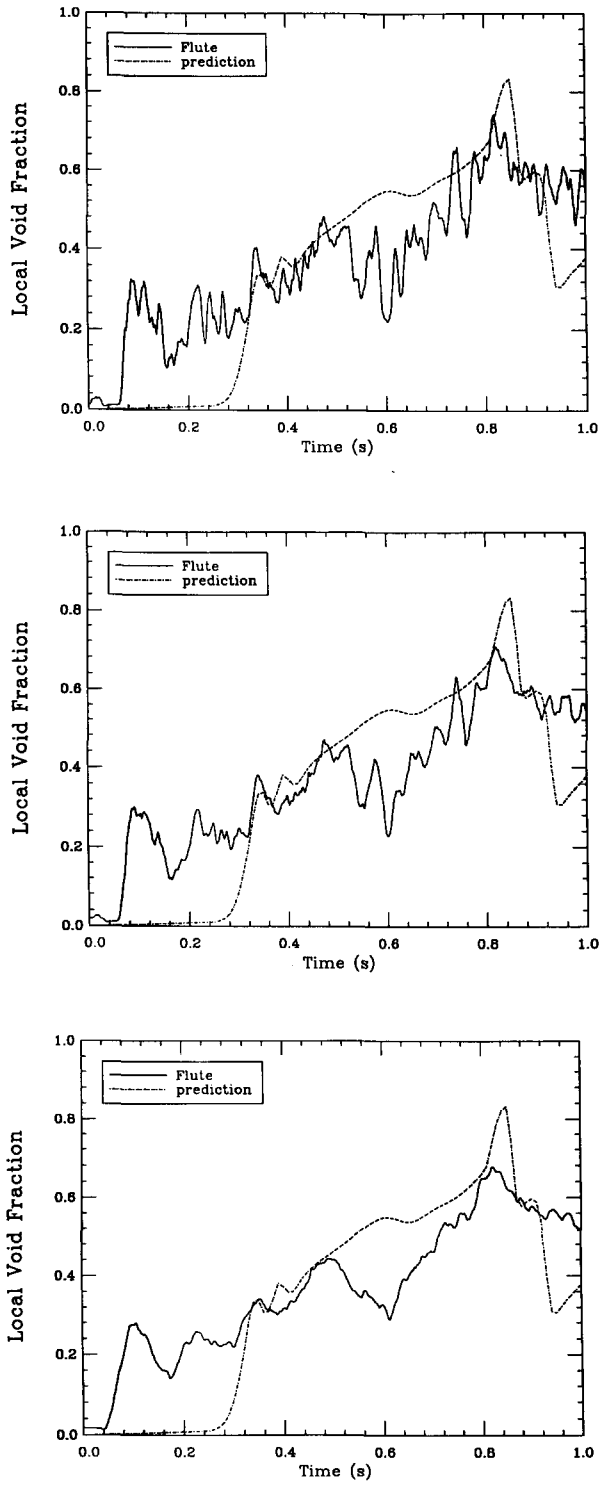

sented here provide only a very initial quantification; however, the water depletion phenomenon, in general, seems to be firmly established now.

6. Acknowledgments

This work was supported by the U.S. Nuclear Regulatory Commission under Contract No. 04-89-082.

7. References

[1] R.E. Henry and H.K. Fauske, Required initial conditions for energetic steam explosions, in: Fuel–Coolant Interactions, HTD-V19, American Society of Mechanical Engineers (1981).

[2] T.G. Theofanous, B. Najafi and E. Rumble, An assessment of steam-explosion-induced containment failure; Part I: Probabilistic aspects, Nucl. Sci. Engng. 97 (1987) 259–281.

[3] W.H. Amarasooriya and T.G. Theofanous, Premixing of steam explosions: a three-fluid model, Nucl. Engng. Des. 126 (1991) 23–39.

[4] C. Liu, T.G. Theofanous and W.W. Yuen, Film boiling from spheres in single- and two-phase flow, 1992 National Heat Transfer Conference, San Diego, August 9–12, 1992.

[5] S. Angelini, W.M. Quam, W.W. Yuen and T.G. Theofanous, FLUTE: FLUorescent TEchnique for two-phase-flow liquid-fraction measurements, Proc. 1991 ANS Winter Meeting, San Francisco, CA, November 1991.

[6] H. Yan, W.W. Yuen and T.G. Theofanous, The use of fluorescence in the management of local liquid content in transient multiphase flows, Proc. NURETH-5, Salt Lake City, UT, September 1992, Vol. V, 1271–1278.

[7] T.G. Theofanous, W.W. Yuen, S. Angelini, X. Chen and E. Takara, Steam Explosions: Fundamentals and Energetic Behavior, to be published as NUREG/CR-5960.

Fig. 13. The local void fraction transient obtained by averaging the time-smoothed signals (obtained as in Figs. 11 and 12) of 9 similar runs.